Analysis of Short Pulse Impacting on Microwave Induced Thermo-Acoustic Tomography

Shuangli Liu[1], Zhiqin Zhao[1, *], Xiaozhang Zhu[1], Zhanliang Wang[2], Jian Song[1], Bingwen Wang[1], Yubin Gong[2], Zaiping Nie[1], and Qing-Huo Liu[3]

Abstract—Microwave induced thermo-acoustic tomography (MITAT) is a developing technique for biomedical applications, especially for early breast cancer detection. In this paper, impacts of short microwave pulse on thermo-acoustic (TA) signals are analyzed and verified through some experimental comparisons. In these experiments, short microwave pulses with widths of 10 ns and 500 ns are employed as radiation resources. TA signals generated from a cubic sample are analyzed in both time- and frequency-domain. A trapezoid sample is also performed for experimental comparing. Different from previous literature, the effects of rising edge of radiation microwave pulse have been intensively studied. Experimental results demonstrate that shorter rising edge duration conducts broader bandwidth of TA signal, which give rise to better spatial resolution for tomography imaging.

1. INTRODUCTION

It has been recognized that tissue radiated by pulsed microwave can generate acoustic signals in lossy media since 1970s [1]. Due to different dielectric properties between cancerous and normal tissues, microwave induced thermo-acoustic signals provide the possibility of early detection of breast cancer [2–4]. Significant progresses on both experiment and theory for MITAT have been made in the past three decades [5–7]. On account of the difficulty of system development, the advantages of MITAT on high contrast and high resolution are usually proved in theory or numerical simulations.

In early investigations, it was reported that the spatial resolution depended on the pulse width of microwave source when all the other conditions were identical [8, 9]. Reference [8] showed that the resolution could be improved by employing broader-band ultrasonic transducers and shorter microwave pulses in simulated and experimental way with 0.5 μs. Similar conclusion was also drawn by Wang et al. through experiments with different pulse widths [9]. Nevertheless, there was no experimental verification on shorter pulse, i.e., ten nanosecond level microwave pulse. Impacts of pulse waveform, width and target size on imaging quality were theoretically investigated in [10], in which a conclusion was made that shorter pulse width would lead better imaging resolution. Reference [11] verified that spatial resolution of TA images would decrease with the increment of the excitation pulse width in the long pulse region. X. Da et al. employed microwave pulses of 10 ns and 450 ns to radiate phantoms and copper wires. Very good resolution was achieved [12]. However, deeper analysis on the relationship between ultra-short microwave pulse signals and TA signals were not mentioned. For the relationships between the radiation pulse and the spatial resolution, researches of photoacoustic have developed a lot. Reference [13] indicated that the photoacoustic pressure in one, two and three dimensions can be founded as mappings of the optical deposition of heat in space for short optical radiation pulses. It means information can be found from the shape of the photoacoustic waveform. Besides, a raster-scan

* Corresponding author: Zhiqin Zhao (zqzhao@uestc.edu.cn).
[1] School of Electronic Engineering, University of Electronic Science and Technology of China, Chengdu, Sichuan 611731, China.
[2] School of Physical Electronics, University of Electronic Science and Technology of China, Chengdu, Sichuan 611731, China. [3] Department of Electrical and Computer Engineering, Duke University, Durham, NC 27708, USA.

acoustic resolution broadband optoacoutic mesoscopy was shown in [14]. They investigated the imaging performance using ultrasonic frequency up to 125 MHz. It was the first experimental demonstration of the effect of laser pulse width on the generated optoacoustic signals at high frequencies.

In this paper, further verification of short microwave pulse of 10 ns width impacting on MITAT is investigated. As a comparison, a microwave pulse of 500 ns width is also used in the experiments. Different from previous literature, the effects of rising edge of radiation microwave pulse have been studied. The relationship between microwave pulse width with respect to rising edge and image quality is analyzed. Experimental results demonstrate that narrower rising edge conducts broader bandwidth of TA signal, giving better tomography image.

The remainder of this paper is organized as follows. The relationship between TA signal and rising edge of microwave pulse is analyzed through some simulations and some experimental data in Sec. 2. Several experiments are conducted in Sec. 3 to investigate the effects of rising edge of microwave pulses. TA signals generated from a cubic sample are analyzed in both time- and frequency-domain. And a small trapezoid sample is also used for imaging. Conclusions are drawn in the final section.

2. THEORY AND METHOD

It has been mentioned that pulses of nanosecond-range duration that can carry hundreds of millijoule energy are ideal for obtaining good signal-to-noise ratio (SNR) and spatial resolution in many biological imaging applications [15]. The amplitude of TA signal is proportional to the pressure caused by thermal expansion. The generation of TA pressure $p(\vec{r}, t)$ can be described as [16]

$$\left(\nabla^2 - \frac{1}{c} \frac{\partial^2}{\partial t^2} \right) p(\vec{r}, t) = -\frac{\beta}{C_p} \frac{\partial H(\vec{r}, t)}{\partial t}, \tag{1}$$

where $H(\vec{r}, t)$ is the instantaneous power absorption density, and c, β, C_p are sound speed, isobaric volume expansion coefficient and heat capacity, respectively. The solution of (1) can be written with the integration performed over the imaged volume V as [17]

$$p(\vec{r}, t) = \frac{\beta}{4\pi C_p} \int_V \frac{\partial H(\vec{r}', t')}{\partial t'} \frac{d^3 \vec{r}'}{|\vec{r} - \vec{r}'|} \Big|_{t'=t-|\vec{r}-\vec{r}'|/c}, \tag{2}$$

where $\vec{r}'$ is a spatial location inside the sample and $\vec{r}$ the spatial location of the position where the pressure field is evaluated.

For simplicity, the power deposition function can be separated into spatial and temporal components,

$$\frac{\partial H(\vec{r}', t')}{\partial t'} \approx H_r(\vec{r}') \frac{dH_t(t')}{dt'}, \tag{3}$$

where $H_t(t')$ is the time-domain profile of the microwave pulse and $H_r(\vec{r}')$ the energy-absorption per unit volume of tissue at position $\vec{r}'$, which is proportional to the microwave absorption coefficient of the tissue at position $\vec{r}'$.

Usually, if the microwave pulse duration is short enough to the size of the desired resolution-limited voxel, one can assume the excitation be a delta function in time domain, i.e.,

$$H_r(\vec{r}') \frac{dH_t(t')}{dt'} \approx H_r(\vec{r}') \delta(t'), \tag{4}$$

Duration time (i.e., pulse width) and rising edge are two key parameters for a pulse. However, microwave pulse used in experiment is not an ideal pulse. Therefore its differential with respect to time is not an ideal delta function.

On account of $H_r(\vec{r}')$ given in [15], the generated TA pressure can be rigorously solved as

$$p(\vec{r}, t) = \frac{\beta \sigma}{8\pi C_p} \int_V |\vec{E}(\vec{r}')|^2 H_t'(t') \frac{d^3 \vec{r}'}{|\vec{r} - \vec{r}'|} \Big|_{t'=t-|\vec{r}-\vec{r}'|/c}, \tag{5}$$

where σ is the electric conductivity, $E(\vec{r}')$ the electric field inside the tissue, and $H_t'(t')$ the time derivative of $H_t(t')$. Thus we can obviously find that TA pressure depends on the time derivative of the microwave pulse, i.e., the rising edge of the pulse.
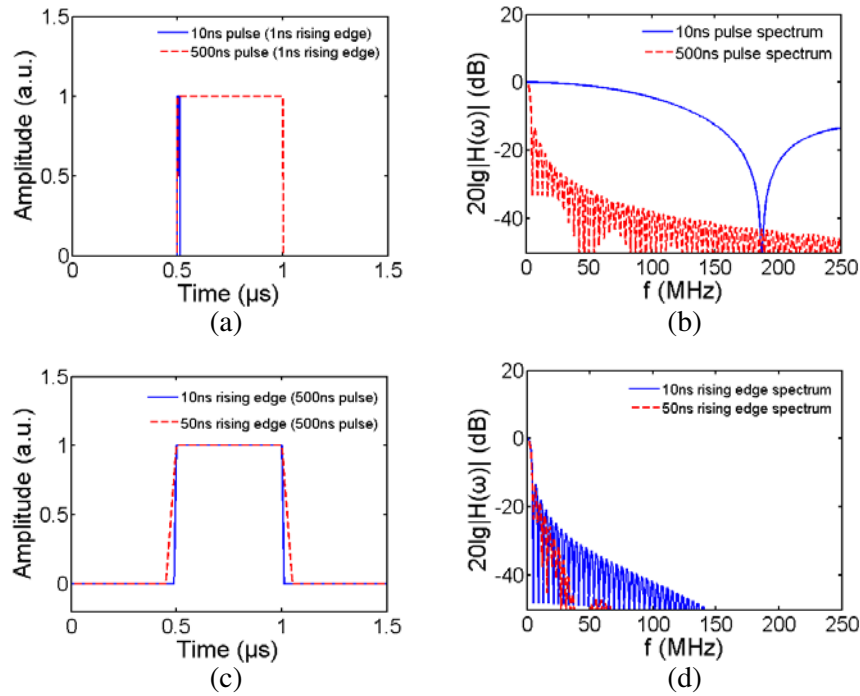
Figure 1. The relationships between different microwave pulses and their spectra. (a) Microwave pulses of same rising edge and different pulse widths; (b) the corresponding spectra of signals in (a); (c) microwave pulses of same pulse width and different rising edges; (d) the corresponding spectra of signals in (c).

Figure 1 shows the relationship between different microwave pulses and their spectra by numerical simulations. Fig. 1(a) indicates that two microwave pulses of different pulse widths and same rising edge; Fig. 1(b) depicts their corresponding spectra. From Fig. 1(b), we can see that the main lobe width of the spectrum of 10 ns pulse is nearly 50 times wider than 500 ns pulse, which is proportional to the pulse width. In addition Fig. 1(c) denotes two microwave pulses of different rising edges and same pulse width; their spectra are also shown in Fig. 1(d). The rising edge duration of an ideal pulse is 0 which will result in an infinite bandwidth. For a practical microwave pulse, the shorter rising edge duration will conducts broader bandwidth, in which high frequency components will contribute more to signal.

Figures 2(a) and (b) indicate a Gaussian pulse and the corresponding TA signal. Actually, the time interval of TA signal is also related to the target radius. From Fig. 2(c), it can be seen that the time intervals decrease as the target radiuses decrease conditioning that the radiated microwave pulse is same.

(c)
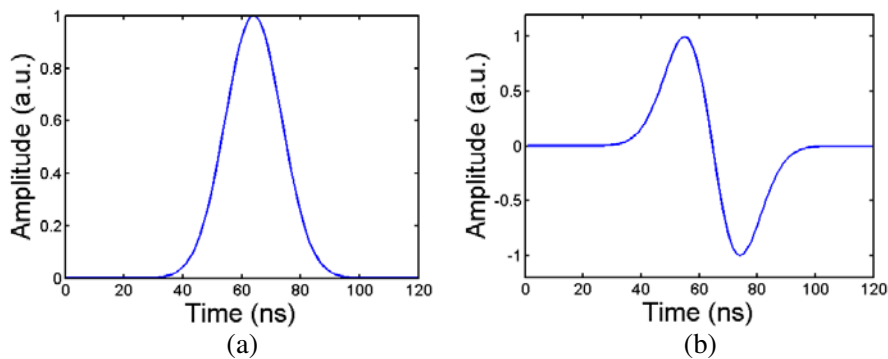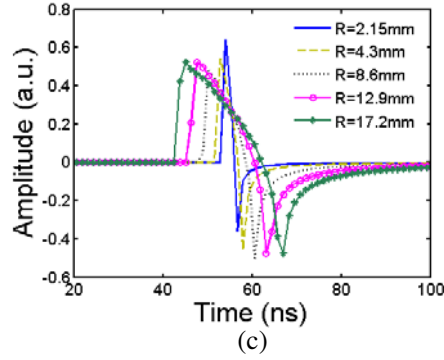
Figure 2. (a) A microwave pulse of Gaussian profile; (b) corresponding TA signal of the Gauss pulses in (a); (c) TA signals with different sample radiuses.

(a)   (b)

(c)   (d)
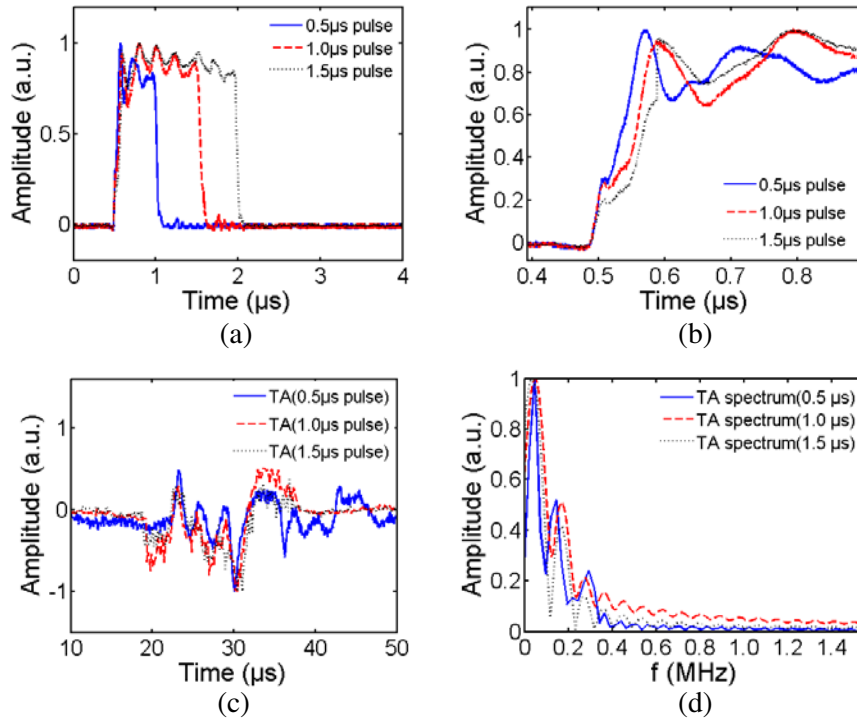
Figure 3. The impacts of microwave pulses on TA signals for different pulse widths. (a) Microwave pulses; (b) details of the rising edge of three different pulses; (c) TA signals; (d) Corresponding spectra of the TA signals.

The impacts of microwave pulses on TA signals for different pulse widths, i.e., 0.5 µs, 1.0 µs, and 1.5 µs are shown in Fig. 3 (Experimental setup will be given in Sec. 3.). Fig. 3(a) shows the microwave pulses. Fig. 3(b) is enlarged details of the rising edges of the pulses in Fig. 3(a). The rising edges of the 3 pulses are very similar. Generated TA signals are shown in Fig. 3(c). Fig. 3(d) gives the corresponding spectrum of the three TA signals. It shows that the spectra of the TA signals have little difference even with different pulse widths.

3. EXPERIMENTS AND DISCUSSIONS

In order to demonstrate the impacts of short microwave pulse on TA signals, especially the effect of rising edge, some experiments are conducted. In the experiments, short microwave pulses with widths

of 10 ns and 500 ns are employed as radiation resources while TA signals are analyzed in both time- and frequency-domain.

3.1. Experimental Setup

Due to the effectiveness of simulating the real tissue with the phantom, experimental samples which have similar electronic parameters with tumor were made from 2.4% agar, 2% salt and 95.6% deionized water [18, 19]. A cubic sample with a size of $1\,\text{cm} \times 1\,\text{cm} \times 1\,\text{cm}$ is shown in Fig. 4(a). Fig. 4(b) shows a sketch map of the MITAT system which has been illustrated in [20, 21]. The pulse width of the microwave generator is adjustable. It can generate microwave pulse with widths of 10 ns, 0.5 µs,
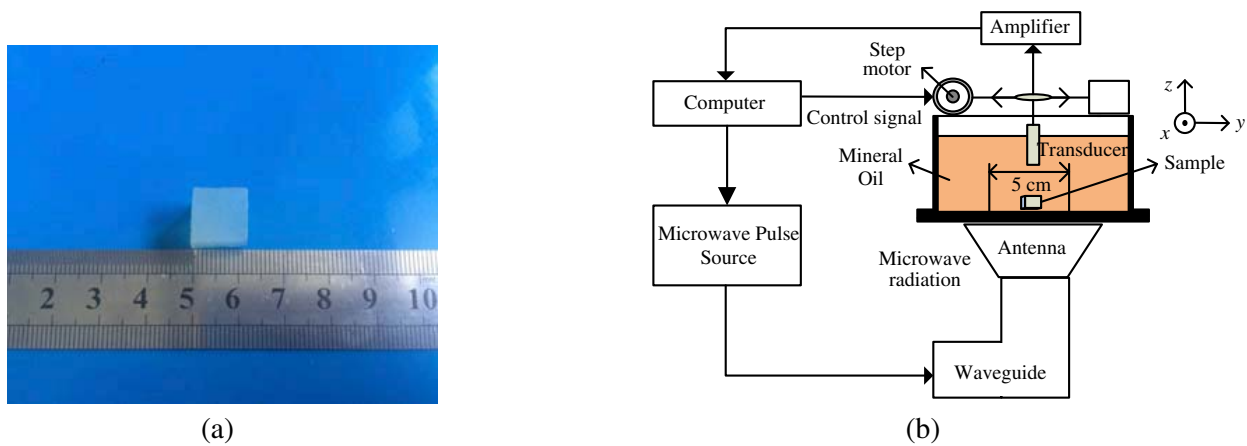
Figure 4. Experimental setup. (a) Experimental sample; (b) Sketch map of the MITAT system.
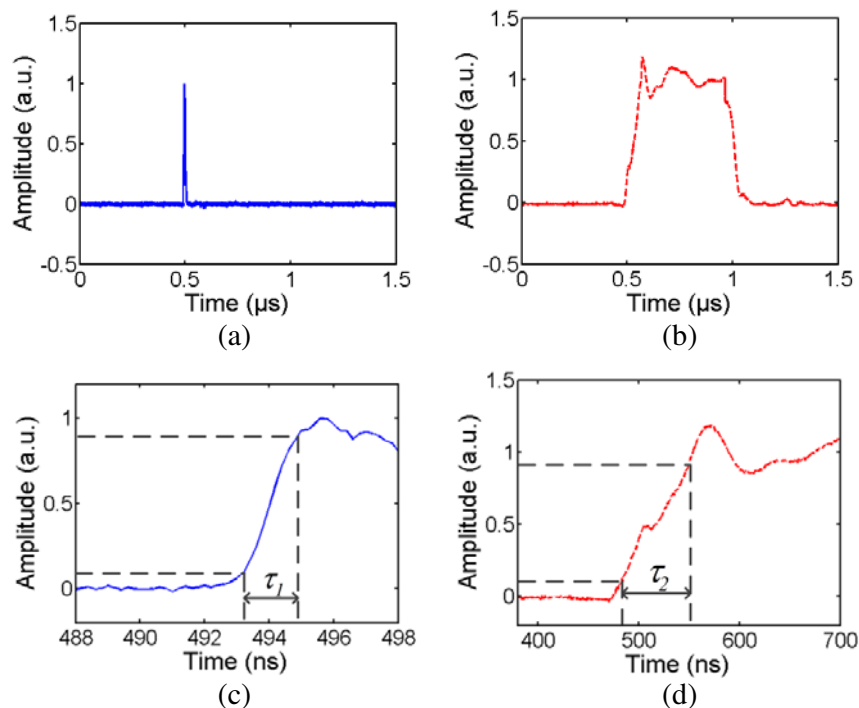
Figure 5. Experimental microwave pulses with different pulse widths. (a) 10 ns pulse in time-domain; (b) 500 ns pulse in time-domain; (c) enlarged rising edge of 10 ns pulse; (d) enlarged rising edge of 500 ns pulse.

1.0 µs, and 1.5 µs. In order to further demonstrate the image results by using different pulses, a linear transducer array is developed to collect TA signals. The data collection system has five main parts: 1) a container which is full of mineral oil; 2) a transducer (V314-SU, Olympus) with the center frequency 1 MHz; 3) a step motor; 4) a low noise amplifier (Panametrics-NDT 5662, Olympus); and 5) a computer. Microwave pulse radiates upward from the bottom of the container. Setting the center of the container as the origin, the transducer moves ±2.5 cm along y axis to realize linear scanning. The system collected data at every 0.5 mm, thus 100 sets of data were collected to do image processing.

Figures 5(a) and (b) show two generated microwave pulses in experiments, one is 10 ns and the other is 500 ns. Enlarged details of the rising edges of pulses are given in Figs. 5(c) and (d). The rising edge duration time of 10 ns pulse from about 493.2 ns to 494.8 ns is 1.6 ns versus 64.1 ns rising edge duration of 500 ns pulse which is from 494.7 ns to 558.8 ns.

3.2. Experimental Results and Analyses

Figures 6(a) and (b) give the TA signals in time domain which are generated from the cubic sample illuminated by two microwave pulses as shown in Fig. 5 and take the average of 100 sets of data to improve the SNR although they are also interfered by noise. Figs. 6(c) and (d) denote short time Fourier transform (STFT) of signals in Figs. 6(a) and (b), which adopts Hamming window of 256 points. Joint time and frequency analyses reflect real TA signals lasting time. In Fig. 6(c), the actual TA signal minimum duration can reach 2.3 µs and TA signal produced by 500 ns pulse will be at least 12.08 µs. According to the relationship between the time domain and the frequency domain, the bandwidth of TA signal of 10 ns is about 5.2 times wider than the bandwidth of TA signal radiated by 500 ns.

High frequency components are included in the rising edge of microwave pulse. And these high frequency components significantly contribute to induced TA signals. According to (5) from the theoretical analyses, sound pressure relates time derivative of time-domain profile of the microwave
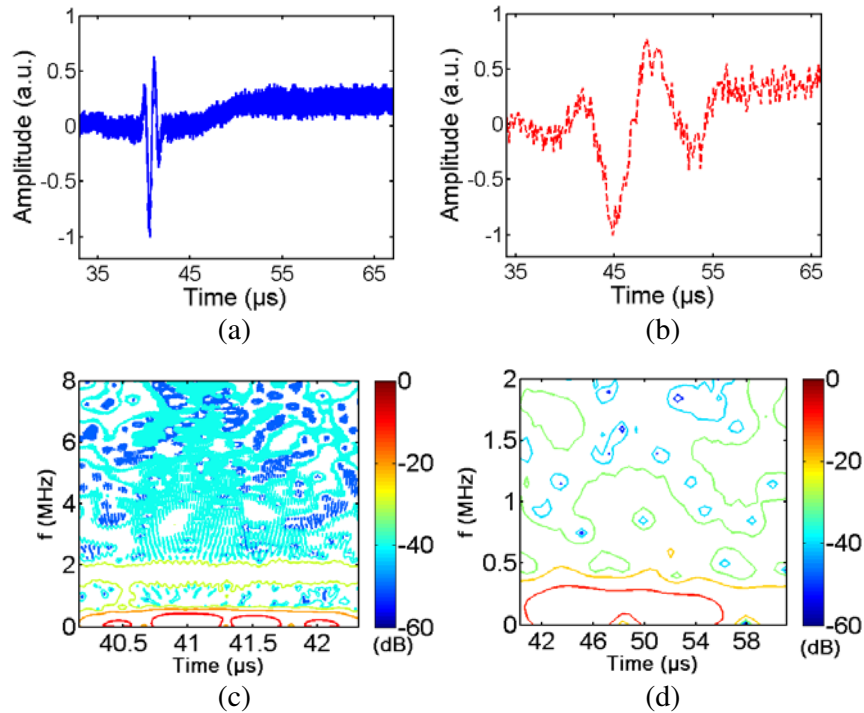
Figure 6. Experimental results for time- and frequency-domain profiles of TA signals produced from a cubic sample. (a) Time-domain waveform of TA signal produced by 10 ns pulse; (b) time-domain waveform of TA signal produced by 500 ns pulse; (c) STFT of TA signal in (a); (d) STFT of TA signal in (b).

pulse and energy-absorption per unit volume of tissue, which is also named specific absorption rate. For input microwave pulses, the ratio between the slope rates of rising edges of the 10 ns pulse and the 500 ns pulse is about 79.88, whereas the ratio of their corresponding energy absorption rates is about 0.066. Thus the sound pressure generated by 10 ns is about 5.27 times wider than 500 ns. This means that the experimental results agree well with the theoretical analyses in Sec. 2.

Due to its high performance in imaging, time reversal mirror (TRM) [22, 23] method is applied to synthesize an image.

Figure 7 is the reconstructed images of the cubic sample radiated with different microwave pulses. The images are normalized according to their own maximum values. The dotted squares stand for the real shape of the cube in yoz plane. In both Figs. 7(a) and 7(b), the cube has been imaged with two clear boundaries corresponding to the two sides of the target. The distance between the two boundaries is about 1.2 cm, which is very close to the real size of the cube. Obviously, Fig. 7(a) has better resolution than that of Fig. 7(b) due to wider spectrum of the TA signal generated from 10 ns pulse as demonstrated in Figs. 6(c) and (d).

In order to quantitatively analyze spatial resolutions the results generated from different pulses, pressure profiles of the two boundaries of the cubic sample are compared in Fig. 8. The solid line represents the amplitude profile of the image in Fig. 7(a) along z axis across the center. The dashed line is the amplitude profile of the image in Fig. 7(b) along z axis across the center. The amplitudes of the two profiles are normalized.

Each pressure profile has two peak values, corresponding to the two edges of the target. The top boundary occurs at $z = 32$ mm, the bottom boundary of the 10 ns profile is at the position of $z = 45.2$ mm versus the position at $z = 43.6$ mm for the 500 ns profile. The corresponding size of the sample along the z axis is about 13.2 mm and 11.6 mm, respectively. Both are close to the real size of

(a) (b)
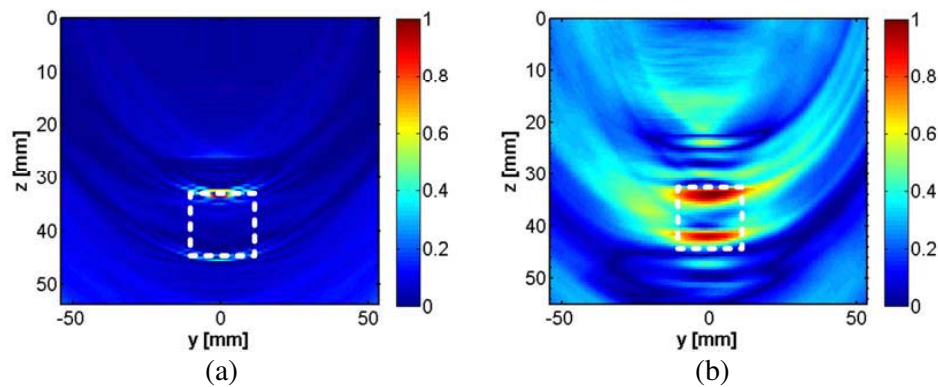
Figure 7. Experimental images for cube sample. (a) Result by using 10 ns pulse; (b) result by using 500 ns pulse.
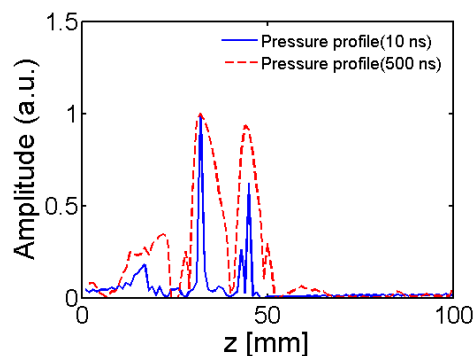
Figure 8. Profiles of pressure along the vertical center of the cube sample.
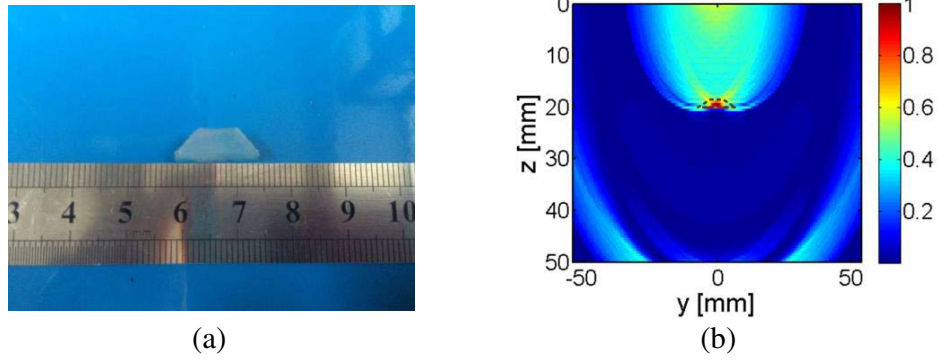
Figure 9. (a) Trapezoid sample used for comparison; (b) experimental result by 500 ns pulse.

the target. Besides, according to the Rayleigh criterion, the ratio of the two spatial resolutions is about 4.91, which agrees with the ratio of 5.27 as analyzed in Sec. 3.2.

In order to further demonstrate the image results, a trapezoid sample with size of $0.5\,cm \times 1.5\,cm \times 0.5\,cm$ is also used for imaging as shown in Fig. 9.

The resolution of the images depends on the available frequency content of the ultrasonic signals. It is determined by the radiation signals, the acoustic attenuation, the frequency response of the transducer and the phase distortion because of the acoustic velocity heterogeneities [24, 25]. To demonstrate the relationship between the radiation microwave pulses especially the rising edge duration and the resolution of the image, we assume that acoustic propagates in a homogeneous medium because the experimental conditions are same except the microwave pulses. It was shown that the amplitude distortion in the breast TAT is minor under the assumption of the homogeneous distribution of sound [25]. And phase distortion can be compensated for when complete or partial information on the distribution of acoustic velocity in the breast is included in the reconstruction methods [25]. Besides, narrower bandwidth of the transducer will lead to TA signal narrower bandwidth which was shown in [8]. And the bandwidth of the transducer we used in the experiments covers both bandwidths of the TA signal induced by 10 ns and 500 ns. So the resolution depends on the microwave pulse especially the rising edge when the detectors are same. Therefore, the experiments match well with the theoretical analysis. Narrower rising edge microwave pulse conducts better spatial resolution.

4. CONCLUSIONS

In this paper, the impacts of short microwave pulse (10 ns) on TA signals, especially the effect of rising edge, are analyzed and further verified through some experiments. The relationship between different microwave pulses and their spectra are numerically simulated. It is demonstrated that shorter rising edge duration gives rise to broader bandwidth. The impacts of microwave pulses on TA signals for three different pulses of the same rising edge are showed through experimental data. The experimental comparisons show that shorter pulse microwave source can conduct broader bandwidth TA signal. And the analyses demonstrate that the rising edge of the microwave pulse contributes more high frequency components. Reconstructed images show that TA imaging with shorter microwave pulse achieves better spatial resolution due to broader spectrum of the generated TA signal. Quantitative analyses of the experimental results are in good accordance with the theoretical predication and simulation results. Both theoretical and experimental analyses in this paper validate that the width of rising edge of radiation pulse is crucial in MITAT.

ACKNOWLEDGMENT

REFERENCES

1. Lin, J. C., "On microwave-induced hearing sensation," *IEEE Trans. Microw. Theory Techn.*, Vol. 25, 605–613, 1977.

2. Lazebnik, M., D. Popovic, L. McCartney, C. B. Watkins, M. J. Lindstrom, J. Harter, S. Sewall, T. Ogilvie, A. Magliocco, and T. M. Breslin, "A large-scale study of the ultrawideband microwave dielectric properties of normal, benign and malignant breast tissues obtained from cancer surgeries," *Phys. Med. Biol.*, Vol. 52, No. 20, 6093, 2007.

3. Catapano, I., L. Di Donato, L. Crocco, O. M. Bucci, A. F. Morabito, T. Isernia, and R. Massa, "On quantitative microwave tomography of female breast," *Progress In Electromagnetics Research*, Vol. 97, 75–93, 2009.

4. Zastrow, E., S. K. Davis, M. Lazebnik, F. Kelcz, B. D. van Veen, and S. C. Hagness, "Development of anatomically realistic numerical breast phantoms with accurate dielectric properties for modeling microwave interactions with the human breast," *IEEE Trans. Med. Imag.*, Vol. 55, No. 12, 2792–2800, 2008.

5. Wang, L. V., X. Zhao, H. Sun, and G. Ku, "Microwave-induced acoustic imaging of biological tissues," *Rev. Sci. Instrum.*, Vol. 70, No. 9, 3744–3748, 1999.

6. Gao, F., Y. Zheng, X. Feng, and C. D. Ohl, "Thermoacoustic resonance effect and circuit modelling of biological tissue," *Appl. Phys. Lett.*, Vol. 102, No. 6, 063702, 2013.

7. Qin, T., X. Wang, Y. Qin, P. Ingram, G.-B. Wan, R. S. Witte, and H. Xin, "Experimental validation of a numerical model for thermoacoustic imaging applications," *IEEE Antennas Wireless Propag. Lett.*, Vol. 14, 1235–1238, 2015.

8. Ku, G. and L. V. Wang, "Scanning thermoacoustic tomography in biological tissue," *Med. phys.*, Vol. 27, 1195–1202, 2000.

9. Ku, G. and L. V. Wang, "Scanning microwave-induced thermoacoustic tomography: Signal, resolution, and contrast," *Med. Phys.*, Vol. 28, 4–10, 2001.

10. Wang, X., D. R. Bauer, J. L. Vollin, D. G. Manzi, R. S. Witte, and H. Xin, "Impact of microwave pulses on thermoacoustic imaging applications," *IEEE Antennas Wireless Propag. Lett.*, Vol. 11, 1634–1637, 2012.

11. Lou, C., L. Nie, and D. Xu, "Effect of excitation pulse width on thermoacoustic signal characteristics and the corresponding algorithm for optimization of imaging resolution," *J. Appl. Phys.*, Vol. 110, 083101, 2011.

12. Lou, C., S. Yang, Z. Ji, Q. Chen, and D. Xing, "Ultrashort microwave-induced thermoacoustic imaging: A breakthrough in excitation efficiency and spatial resolution," *Phys. Rev. Lett.*, Vol. 109, 218101, 2012.

13. Diebold, G., T. Sun, and M. Khan, "Photoacoustic monopole radiation in one, two, and three dimensions," *Phys. Rev. Lett.*, Vol. 67, No. 24, 3384, 1991.

14. Omar, M., J. Gateau, and V. Ntziachristos, "Raster-scan optoacoustic mesoscopy in the 25–125 MHz range," *Opt. Lett.*, Vol. 38, No. 14, 2472–2474, 2013.

15. Razansky, D., S. Kellnberger, and V. Ntziachristos, "Near-field radiofrequency thermoacoustic tomography with impulse excitation," *Med. phys.*, Vol. 37, 4602–4607, 2010.

16. Rosenthal, A., D. Razansky, and V. Ntziachristos, "Fast semi-analytical model-based acoustic inversion for quantitative optoacoustic tomography," *IEEE Trans. Med. Imag.*, Vol. 29, 1275–1285, 2010.

17. Xu, M. and L. V. Wang, "Time-domain reconstruction for thermoacoustic tomography in a spherical geometry," *IEEE Trans. Med. Imag.*, Vol. 21, 814–822, 2002.

18. Guy, A. W., "Analyses of electromagnetic fields induced in biological tissues by thermographic studies on equivalent phantom models," *IEEE Trans. Microw. Theory Techn.*, Vol. 16, No. 2, 205–214, 1971.

19. Song, J., Z. Zhao, J. Wang, X. Zhu, J. Wu, Z. Nie, et al., "Evaluation of contrast enhancement by Carbon Nanotubes for microwave induced thermo-acoustic tomography," *IEEE Trans. Biomed. Eng.*, Vol. 62, 939–938, 2014.

20. Zhao, Z., J. Song, X. Zhu, J. Wang, J. Wu, Y. Liu, Z.-P. Nie, and Q. H. Liu, "System development of microwave induced thermo-acoustic tomography and experiments on breast tumor," *Progress In Electromagnetics Research*, Vol. 134, 323–336, 2013.

21. Song, J., Z. Zhao, J. Wang, X. Zhu, J. Wu, Z.-P. Nie, and Q. H. Liu, "An integrated simulation approach and experimental research on microwave induced thermo-acoustic tomography system," *Progress In Electromagnetics Research*, Vol. 140, 385–400, 2013.

22. Hristova, Y., P. Kuchment, and L. Nguyen, "Reconstruction and time reversal in thermoacoustic tomography in acoustically homogeneous and inhomogeneous media," *Inverse Problems*, Vol. 24, 055006, 2008.

23. Zheng, W., Z. Zhao, Z.-P. Nie, and Q. H. Liu, "Evaluation of TRM in the complex through wall environment," *Progress In Electromagnetics Research*, Vol. 90, 235–254, 2009.

24. Deán-Ben, X. L., D. Razansky, and V. Ntziachristos, "The effects of acoustic attenuation in optoacoustic signals," *Phys. Med. Biol.*, Vol. 56, No. 18, 6129, 2011.

25. Xu, Y. and L. V. Wang, "Effects of acoustic heterogeneity in breast thermoacoustic tomography," *IEEE Transactions on Ultrasonics, Ferroelectrics and Frequency Control*, Vol. 50, No. 9, 1134–1146, 2003.